Published in final edited form as:
Circ Heart Fail. 2014 January ; 7(1): 184–193. doi:10.1161/CIRCHEARTFAILURE.113.000649.

DSAGE Identifies Osteopontin as a Downstream Effector of Integrin-Linked Kinase (ILK) in Cardiac-Specific ILK Knockout Mice

Jing Dai, MD, PhD[1,2], **Takashi Matsui, MD, PhD**[3], **E. Dale Abel, MD, PhD**[4], **Shoukat Dedhar, PhD**[5], **Robert E. Gerszten, MD**[6,2], **Christine E. Seidman, MD**[7,8], **J. G. Seidman, PhD**[8], and **Anthony Rosenzweig, MD**[1,2]

[1]Cardiovascular Division, Beth Israel Deaconess Medical Center, Boston, MA

[2]Harvard Medical School, Boston, MA

[3]Center for Cardiovascular Research, John A. Burns Sch. of Med., University of Hawaii, Honolulu, HI

[4]Endocrinology Division and Program in Molecular Medicine, University of Utah, Salt Lake City, UT

[5]British Columbia Cancer Research Centre, Vancouver, BC Canada

[6]Massachusetts General Hospital, Boston, MA

[7]Brigham and Women's Hospital, Boston, MA

[8]Department of Genetics, Harvard Medical School, Boston, MA

Abstract

Background—Integrin-linked kinase (ILK) is a serine-threonine kinase that has been linked to human and experimental heart failure, but its role in the heart is not fully understood.

Methods and Results—To define the role of cardiomyocyte ILK, we generated cardiac-specific ILK knockout mice (CSILK-KO) using α-MHC-driven Cre expression. CSILK-KO spontaneously developed lethal dilated cardiomyopathy and heart failure with an early increase in apoptosis, fibrosis, and cardiac inflammation. To identify downstream effectors, we used deep sequence analysis of gene expression (DSAGE) to compare comprehensive transcriptional profiles of CSILK-KO and WT hearts from 10 day old mice before the development of cardiac dysfunction. ~2×10^6 cDNA clones from each genotype were sequenced, corresponding to 33,274 independent transcripts. 93 genes were altered, using nominal thresholds of >1.4-fold change and $p<0.001$. The most highly upregulated gene was osteopontin (47-fold increase, $p=9.6\times10^{-45}$), an inflammatory chemokine implicated in heart failure pathophysiology. ILK also regulated osteopontin expression in cardiomyocytes *in vitro*. Importantly, blocking antibodies to osteopontin mitigated but did not fully rescue the functional decline in CSILK-KO mice.

Conclusions—Cardiomyocyte-specific ILK deletion leads to a lethal cardiomyopathy characterized by cardiomyocyte death, fibrosis, and inflammation. Comprehensive profiling

Correspondence to, Dr. Anthony Rosenzweig, Cardiovascular Division, Beth Israel Deaconess Medical Center, 3 Blackfan Circle, CLS/947, Boston, MA 02215, arosenzw@bidmc.harvard.edu, Tel: 617-735-4241, Fax: 617-735-4202.

Disclosures
None.

identifies ILK-dependent transcriptional effects and implicates osteopontin as a contributor to these phenotypes.

Keywords

integrin-linked kinase; dilated cardiomyopathy; osteopontin; transcript profiling

The serine-threonine kinase, integrin-linked kinase (ILK), was identified as a protein interacting with the cytoplasmic tail of β1 integrins[1]. The ternary complex of ILK, PINCH, and parvin (IPP complex) couples integrins to the actin cytoskeleton[2]. ILK phosphorylates integrin cytoplasmic domains and multiple downstream signaling/cytoskeletal proteins, regulating cascades of integrin-mediated signaling events. This connection to bidirectional integrin signaling raises the possibility that ILK could regulate the heart's response to biomechanical stress. Interestingly, ILK expression is increased in human cardiac hypertrophy[3], and point mutations in ILK associated with dilated cardiomyopathy (DCM) in humans are linked to defects in both endothelial cells and cardiomyocytes in model systems[4]. Moreover, ILK protein complexes are essential components of the cardiac mechanical stretch sensor in zebrafish[5]. These studies provide a genetic link between aberrant ILK function and cardiovascular disease, and underscore the potential relevance and importance of understanding ILK's cardiovascular roles. The current study investigates the physiological roles of ILK in cardiomyocytes through conditional deletion. Whether ILK has kinase-independent activity is controversial[6]. Ablation of ILK in the heart[7], skeletal muscle[8] or nervous system[9] abrogated phosphorylation of Ser473 of Akt, but knock-in mice carrying mutations in the putative PH domain (R211A) or in the autophosphorylation site (S343A or S343D) are completely normal and do not show changes in Akt or Gsk-3β phosphorylation or actin organization downstream of integrins[10]. However, knock-in of K220M, an essential amino acid for ILK kinase activity within the ATP-binding subdomain-2 of the catalytic domain, resulted in severe developmental defects in the kidney[10].

Mice with ILK deletion in both heart and skeletal muscle developed heart failure with disrupted cytoarchitecture and fibrosis, as well as decreased phosphorylation of FAK and Akt, leading the authors to implicate loss of signaling via these pathways as primary contributors to the phenotypes observed[7]. However, genetic deletion of molecules in this pathway including FAK[11], Akt[12, 13], PINCH1[14] or β1-integrin itself[15] have either no or mild cardiac phenotypes at baseline, only developing DCM after biomechanical stress such as aortic constriction. Thus, the much more severe phenotype seen with cardiac and skeletal ILK deletion suggests other unrecognized mechanisms may be playing an important role. Although skeletal muscle appeared normal in these mice, it is difficult to exclude a potential contribution from systemic effects of subtle abnormalities.

Here we report the generation and characterization of cardiac-specific ILK knockout mice. CSILK-KO mice develop a dramatic and early lethal DCM and fibrosis, associated with inflammation and cardiomyocyte apoptosis. To define the downstream mechanisms, we used DSAGE (deep sequence analysis of gene expression)[16], a novel nanotechnology, that enables high-fidelity nucleic acid sequencing at reduced cost to sequence ~2 million cDNA clones from CSILK-KO and control hearts at 10 days postnatally *before* the development of cardiac dysfunction. Interestingly, the single most upregulated transcript was osteopontin (OPN), an inflammatory chemokine previously associated with myocarditis and heart failure[17, 18]. Recent literature[19] and experiments with function-blocking antibodies suggest OPN is an important contributor to the phenotype in CSILK-KOs. Thus the current studies link ILK to previously unrecognized cardiac phenotypes, provide a global transcriptional

profile of the effects of cardiomyocyte ILK deletion, and underscore the importance of Akt-independent effectors in these phenotypes.

Methods

Generation of cardiomyocyte-specific ILK knockout mice

α-Myosin Heavy Chain-Cre (α-MHC-Cre) mice[20] were crossed with homozygous floxed ILK ($ILK^{fl/fl}$) mice[21] to generate cardiac specific ILK knock-out animals (CSILK-KO: α-MHC-Cre^{+}; $ILK^{fl/fl}$), and the α-MHC-Cre^{-} littermates were used as controls (WT: α-MHC-Cre^{-}; $ILK^{fl/fl}$). All mice were on a C57BL/6 background. Genotyping was performed as previously described[21]. Animals were handled in accordance with protocols approved by the BIDMC Subcommittee on Research Animal Care.

Cardiac morphological analyses

Hearts were excised and fixed overnight in 4% paraformaldehyde (PFA). Following progressive dehydration with 20% glucose, heart samples were embedded in paraffin. 8μm sections were subjected to Masson's Trichrome staining fibrosis visualization. Images were collected using a Leica DM IRB microscope and a Leica camera (Leica Microsystems). Quantation of collagen deposition in cross-sections was performed with Photoshop.

Immunohistochemistry and immunofluorescence staining

Immunofluorescent staining of cardiac cryosections from CSILK-KO and control mice (4 each) were performed using the VECTASTAIN ABC Kit (Vector Lab) as described[22] with DAPI (Invitrogen) nuclear conterstaining. The following primary antibodies were used: anti-α-actinin (1:400,Sigma-Aldrich), anti-ILK (1:1000; Upstate), and anti-CD45 (1:100; BD Pharmingen).

Echocardiography

Echocardiography was performed on unanesthetized mice using a 13L high-frequency linear (10 MHz) transducer (VingMed 5, GE Medical Services) with depth set at 1 cm and 236 frames per second for 2D images. M-mode images used for measurements were taken at the mid-papillary muscle level.

Immunoblotting

Cardiomyocyte protein extracts were prepared as described[23]. Protein from 10 to 21 day old mouse hearts was obtained after atria were removed. After concentration determination by the Bradford method (Bio-Rad), proteins (50 μg) were separated by SDS-PAGE on 4–20% gels and transferred to nitrocellulose membranes (Bio-Rad) by semidry transfer. Blots were incubated with anti-ILK (1:1000; Upstate), anti-Osteopontin (1:1000; Santa Cruz), anti-phospho-Ser-473-Akt (1:1000; serine 473; Cell Signaling), anti-GAPDH (1:4000, Cell Signaling) overnight at 4°C and subsequently incubated with horseradish peroxidase (HRP)-conjugated secondary antibody (1:2000; Cell signaling), and detected by chemiluminescence (Cell Signaling).

RNAi

Cells were transfected with Small siRNA duplexes (Applied Biosystems) at 10 nM using lipofectamine RNAimax transfection reagent (Invitrogen). siRNA target ILK sequences (5′ to 3′) were as follows: sense-GUAGUGUAAUGAUCGAUGAtt, antisense-UCAUCGAUCAUUACACUACgg (s139497). Silencer Select Negative Control siRNA was purchased from Applied Biosystems. siRNA transfections were performed in six-well plates and harvested 48 h later.

Quantitative RT-PCR

Total RNA was isolated from cardiac ventricles using TRIzol (Invitrogen) per the manufacturer's recommendations. RNA concentration was determined with a spectrophotometer, and 2μg used to prepare cDNA (Applied Biosystems). mRNA quantitation was performed for validation by quantitative reverse-transcription PCR (QRT-PCR) relative to GAPDH using the ΔΔCT method as described[24]. Primer sequences are listed in the online supplement.

TUNEL staining

TUNEL staining was performed with the ApopTag Plus Fluorescein In Situ Aopotosis Detection Kit (Millipore), according to the manufacturer's recommendations. α-actinin (1:400; Sigma) was used to identify cardiomyocytes (red), and nuclei were counterstained with DAPI (Invitrogen). TUNEL-positive cardiomyocytes were counted in 10 low-power fields from 3 cardiac cryosections of CSILK-KO and controls. More than 1000 nuclei were counted with NIH image J.

DSAGE

Total RNA was prepared from 5 hearts from male mice of each genotype (α-MHC-Cre^{+}/$ILK^{flox/flox}$ and α-MHC-Cre^{-}/$ILK^{flox/flox}$) using Trizol (Invitrogen). RNA from each genotype was pooled in equal proportion to provide 10μg of total RNA for the generation of cDNA libraries[25].

Antibody treatment

Newborn CSILK-KO pups were followed by echocardiography until their fractional shortening was reduced to ~40% and then treated with a neutralizing goal polyclonal OPN IgG (R&D Systems) or control IgG (40μg/10g body weight) by intraperitoneal injection. Mice were sacrificed 8 days after last antibody injection.

Statistics

Values are expressed as mean±SEM. $p<0.05$ was considered significant. Comparisons between two independent groups were performed using unpaired Student's *t*-tests with Welch's correction. Comparisons between two independent cohorts (e.g. WT and CSILK-KO) at multiple time points were performed using two-way ANOVA. Comparisons between two independent groups (e.g. CSILK-KO mice with different antibody treatments) followed with repeated measures were performed using repeated-measure two-way ANOVA. Bonferroni post-hoc procedure was used in both cases. For DSAGE, statistical comparisons of gene expression were performed as previously described[25] using the Audic and Claverie alternative to Fisher's exact test[26]. Kaplan-Meier curves were used to display survival data. The logrank test was used to compare two survival curves.

Results

Cardiac Specific Deletion of ILK

To investigate ILK's role specifically in cardiomyocytes, we generated cardiac-specific ILK knockout mice (CSILK-KO) by breeding α-MHC-Cre^{+} transgenic mice[20] to $ILK^{flox/flox}$ mice[21]. Hearts from CSILK-KO mice had significantly reduced ILK expression at the mRNA and protein level (Figure 1A, B) 10 days postnatally before the development of cardiac dysfunction. As previously reported by others[21], ILK deletion significantly reduced baseline phosphorylation of Akt (Figure 1B). The residual ILK expression seen in whole ventricle extracts, likely reflects expression in non-cardiomyocytes. This was confirmed by immunofluorescent staining for ILK, which revealed no signal in cardiomyocytes from

CSILK-KO hearts but preserved vascular expression (Figure 1C). Normal ILK expression was also seen in other tissues including brain, liver, lung, kidney, skeletal muscle, and intestine (data not shown). Thus the conditional genetic strategy employed produced effective and specific deletion of ILK in cardiomyocytes.

CSILK-KO Mice Exhibit Early Postnatal Mortality and Develop Dilated Cardiomyopathy

CSILK-KO mice were born at the expected Mendelian frequency (data not shown) and had no obvious phenotypic differences compared to littermate controls at 10 days but by 15 days CSILK-KO pups manifested cardiac dilation and dysfunction on echocardiography which became severe by 21 days (Figure 2A, Table). Echocardiographic parameters were consistent with the development of a dilated cardiomyopathy (DCM) including enlarged left ventricular chamber sizes (LVDd and LVDs) starting at 15 days. In addition, the interventricular septum (IVS) and left ventricular poster walls (LVPW) became progressively thinner in CSILK-KO hearts. These changes in cardiac dimensions were accompanied by a striking decline in cardiac function in CSILK-KO mice, with fractional shortening (FS) declining from 61.28±1.38 at 10 days to 8.91±2.12 (Table).

CSILK-KO mice died by 3–6 weeks of age (n=12) (Figure 2A). The median survival for the CSILK-KO mice was 4 weeks, with few mice surviving to 6 weeks, while, as expected, all $ILK^{flox/flox}$ control mice survived over this period. Both heart and lung weights normalized to tibial length were increased compared with controls (Figure 2B), consistent with DCM and heart failure with pulmonary edema. Histopathology of 21 day old CSILK-KO hearts confirmed right and left ventricular enlargement and wall thinning compared to controls (Figure 2C). Baseline cardiac function in heterozygous ILK-KO mice ($ILK^{flox/wt}$, cre^{+}) was normal (data not shown). However, the decrease in cardiac ILK expression in these mice was very modest, suggesting there may be compensatory upregulation from the remaining allele. Thus they do not provide a test of haploinsufficiency.

Increased Cardiomyocyte Death, Fibrosis, and Inflammation in CSILK-KO Hearts

DCM can be associated with myocyte cell death, fibrosis, and inflammation, and we examined CSILK-KO hearts for evidence of these processes from 10 to 21 days after birth. Analysis of confocal images revealed increased numbers of TUNEL positive cardiomyocytes in both atria and ventricles of CSILK-KO hearts when compared with their littermate controls ($ILK^{flox/flox}$) hearts (Figure 3A, B). We also found evidence of increased fibrosis by Masson's Trichrome staining (Figure 3C, D) and leukocyte infiltration by CD45 staining (Figure 3E, F). In each case, the findings progressively increased over this time period. Interestingly, cardiomyocyte apoptosis was significantly increased at 10 days *before* CSILK-KO mice develop cardiac dysfunction (Figure 3A, B). Fibrosis showed a trend toward increasing in 10 and 15 day old CSILK-KO hearts, and was significantly increased at 21 days (Figure 3C, D). Inflammatory cell infiltration was significantly increased by 15 days in CSILK-KO hearts (Figure 3E, F), coinciding with the earliest detectable development of cardiac dysfunction. Thus, ILK deletion in cardiomyocytes leads to the development of apoptosis, fibrosis, and inflammation, preceding or coincident with the development of cardiac dysfunction and prior to the disrupted cytoarchitecture seen in late stage failing CSILK-KO hearts, suggesting these represent primary events in the development of DCM after ILK deletion. Numerous studies have demonstrated that cell death including necrosis, is an important component in the pathogenesis of heart failure[27]. Evans blue staining of cardiomyocytes as an indicator of necrosis was also increased in CSILK-KO hearts (Supplemental Figure 1).

DSAGE (Deep Sequence Analysis of Gene Expression)

We used DSAGE, a novel nanotechnology that facilitates global transcriptional profiling, to compare gene expression in hearts from 10 day old CSILK-KOs and littermate controls to identify changes that precede the development of cardiac dysfunction. Approximately 2×10^6 cDNA clones from each genotype (5 hearts for each) were sequenced, corresponding to 33,274 independent transcripts. 93 differentially expressed transcripts were identified with a fold change >1.4 and $p<0.001$, thresholds previously shown to identify relevant effector pathways while minimizing false discovery[16]. The 1.4-fold number represents a practical limit below which QRT-PCR assessment of differences becomes technically challenging to the point where we would prioritize other candidates. Twenty-five transcripts identified by DSAGE were assessed by QRT-PCR, and 16 of these DSAGE candidates were confirmed at $p<0.05$ (Figure 4). In some cases, the failure to validate may reflect a lack of statistical power to detect modest differences by QRT-PCR with 5 samples in each group. The single most highly upregulated transcript on both the DSAGE and QRT-PCR was osteopontin (OPN), which was 47-fold up in 10 day old CSILK-KO hearts by DSAGE ($p=9.6\times10^{-45}$) and 54-fold up ($p < 0.04$) by QRT-PCR.

OPN expression is regulated by ILK, but not by AKT

OPN, also known as Spp1 or Eta-1[28], is an inflammatory chemokine that induces leukocyte infiltration and increases in a variety of cardiovascular diseases including hypertrophy[29], heart failure[18], and myocarditis[17,30]. Interestingly, recent work demonstrates that cardiomyocyte expression of OPN is sufficient to induce DCM associated with inflammatory infiltrates, cardiomyocyte apoptosis, and fibrosis[19]. Thus the dramatic upregulation of OPN could contribute to the phenotypes observed after ILK deletion.

To explore this possibility further, we examined the timing of OPN RNA and protein expression in more detail. As noted above, OPN RNA expression was dramatically increased in CSILK-KO hearts before they develop abnormalities, and continued to increase at post-natal days 15 and 21, while expression in control littermates remained consistently low throughout this period (Figure 5A). OPN protein level also increased early, significantly so by 15 days and further increased by day 21 in CSILK-KO hearts (Figure 5B).

To examine whether ILK regulates OPN expression in cardiomyocytes, we used siRNA to knockdown ILK in rat neonatal cardiomyocytes. QTR-PCR and Western blotting demonstrated reduced ILK mRNA and protein expression as well as increased OPN expression after transfection with an ILK-specific siRNA (Figure 5C, D). Thus, reduced ILK leads to increased OPN expression in isolated cardiomyocytes in the absence of heart failure or other phenotypes that might induce OPN indirectly.

To test whether the increased OPN seen in CSILK-KO hearts contributes to the development of heart failure, we treated CSILK-KO mice with neutralizing OPN antibodies. CSILK-KO mice were followed by echocardiography until their fractional shortening declined to ~40% (generally 14–18 days old) and then were injected intraperitoneally with a neutralizing anti-mouse OPN polyclonal goat IgG or control goat IgG every other day. Echocardiograms performed prior to each injection demonstrate that injection of the OPN-specific antibody mitigates the functional decline in CSILK-KO mice (Figure 6) in comparison to control IgG-injected animals. Not surprisingly given *in vivo* IgG injection across species, the improvement was only transient with a subsequent decline in function that paralleled control-IgG injected CSILK-KO mice. Nevertheless these data support the hypothesis that the dramatically increased OPN expression seen in CSILK-KO mice is contributing to cardiac dysfunction.

To determine whether loss of Akt1 activation contributes to the increased OPN expression seen after ILK deletion, we examined ventricles from Akt1 KO mice[12]. Of note, as reported by others, Akt1 KO mice have a very different phenotype[12,13] compared to CSILK-KO, with essentially normal baseline cardiac function and no evidence of fibrosis, inflammation, or apoptosis at baseline, although they do worse than WT mice after stress[31]. Neither OPN mRNA nor protein expression was altered in 4 week old Akt1 knockout mice[12] (Figure 7). Thus it is unlikely that the marked increase in OPN expression seen in CSILK-KO hearts is due to reduced Akt1 activation.

Discussion

Integrin-linked kinase (ILK) is an adaptor and serine-threonine kinase that links integrins with intracellular cytoskeletal elements and kinase signaling cascades. ILK mutations are associated with human DCM, and previous work suggested a role for ILK in preserving cardiac cytoarchitecture and FAK/Akt signaling[7]. However, the mild baseline phenotypes seen with genetic deletion of FAK and Akt, suggested other important contributors and prompted us to generate cardiac specific ILK knockout mice.

We found that cardiomyocyte-specific ILK deletion led to a severe and lethal dilated cardiomyopathy phenotype, which was even more dramatic than that previously reported for MCK-Cre-driven deletion where the median age of death was 8 weeks[7] compared to 4 weeks in our cohort. The more severe phenotype observed may reflect differential timing and effectiveness of ILK deletion with αMHC-Cre, and is consistent with the suggestion by White[7] that skeletal muscle deletion did not contribute to the DCM phenotype they observed.

We noted cardiac fibrosis in CSILK-KO hearts as previously reported but also found a significant increase in cardiomyocyte cell death that *preceded* the development of cardiac dysfunction or cytoarchitectural abormalities, as well as early infiltration of inflammatory leukocytes, neither of which were previously noted[7]. The timing of these histological phenotypes suggested they may play an early mechanistic role rather than simply being secondary consequences of disrupted cell-cell or cell-matrix interactions[7]. Although baseline Akt phosphorylation was also decreased early in CSILK-KO hearts, both Akt germline knockouts and FAK cardiac knockouts have essentially normal function at these ages suggesting other pathways play an important role.

To identify other contributors to these phenotypes, we performed genome wide transcript profiling of 10 day old hearts from CSILK-KOs and wildtype controls. We chose this time point because it precedes the development of cardiac dysfunction and thus would less likely be confounded by transcriptional effects of the altered phenotypes. Transcript profiling was performed using DSAGE, a recently developed approach that enables sequencing 10^6 to 10^7 tags at low cost with a ~100-fold improvement in sensitivity and speed by using parallel rather than serial analyses[16]. In addition to the improved fidelity for low-abundance transcripts, the large number of independent clones sequenced using DSAGE provides more robust statistical comparisons[16]. DSAGE revealed differential expression of 93 transcripts. The single most upregulated transcript was OPN (Spp1), an inflammatory chemokine previously noted to increase in cardiac hypertrophy and heart failure[18, 30].

Multiple cell lineages present in the failing heart can express OPN. OPN has been identified in rat cardiac fibroblasts, where it contributes to angiotensin II-induced remodeling[32]; in cardiomyocytes[33]; and in macrophages with inflammation[34]. Graf et al. report that cardiomyocytes are a prominent source of OPN *in vivo* both in rat and in humans[30]. PPAR$\gamma^{-/-}$ cardiomyocytes have increased OPN expression, which contribute to macrophage

accumulation within the myocardium[35]. Moreover, diabetes also increases OPN protein levels in the myocardium[36]. Whether there are distinct functional effects of OPN expressed by cardiomyocytes as compared to fibroblasts is not clear but it seems likely that the secreted signal recruits a similar target population of inflammatory cells in both cases. Cardiomyocyte-specific expression of OPN is sufficient to induce a lethal DCM associated with apoptosis, fibrosis, and inflammation[19] similar to that observed after ILK-deletion albeit with a somewhat delayed onset. Interestingly, ongoing OPN expression was required for maintenance of the inflammation and lethal cardiomyopathy phenotype[19], raising the possibility that inhibiting OPN could have a therapeutic benefit in some settings. Consistent with this hypothesis, treatment of CSILK-KO mice with a neutralizing antibody to OPN transiently shifted the decline in cardiac function. Unfortunately the only neutralizing OPN antibody available is a goat polyclonal so the transience of mitigation could reflect either immunological clearance of the foreign antibody by the host or a contribution of OPN-independent factors to cardiac dysfunction.

OPN appears to have multiple effects which include modulating fibroblast and myocyte adhesion to the matrix, matrix synthesis, and synergism with other profibrotic molecules[37]. Two studies have demonstrated that OPN can induce MMP-2 and MMP-9 activation through a NF-κB dependent mechanism[38,39]. We examined MMP activity by gelatin zymography in CSILK-KO hearts as well, and found MMP-2 activity was increased in mice with heart failure but not before the development of cardiac dysfunction (Supplemental Figure 2A, B). These data suggest the increased MMP activity is unlikely to be a primary cause of the DCM phenotype in this model.

ILK has been reported to regulate inflammation in tissue-specific ways. Loss of ILK from mouse hepatocytes results in acute hepatitis, with a variety of pathological findings including inflammation, fatty change, apoptosis, abnormal mitoses, and necrosis[40]. ILK knockdown impaired LPS-mediated endothelial activation by preventing the induction of ICAM-1 and VCAM-1[41]. In contrast, ILK plays a pro-inflammatory role in intestinal inflammation, through effects on chemokine expression, the extracellular matrix and immune tolerance[42].

Our results confirm previous findings with heart and skeletal muscle ILK deletion[7] but extend them in several important ways. First, the similar though more severe phenotype observed with cardiac-restricted deletion suggest (as postulated by White and colleagues[7]) that skeletal muscle deletion is not an important contributor to the DCM phenotype. Second, we document previously unreported phenotypes including cardiomyocyte apoptosis, necrosis, and inflammation in hearts after ILK deletion. Finally, genome-wide transcript profiling identified marked upregulation of the inflammatory chemokine, OPN, early after ILK deletion, before the development of cardiac dysfunction or structural abnormalities. The other differentially regulated transcripts provide a comprehensive overview of ILK-dependent gene expression in the heart that should provide a helpful foundation for future investigation. Taken together, these results support a previously unrecognized connection between ILK and cardiac inflammation, mediated through regulation of OPN expression. We hypothesize that the rapidly lethal DCM observed after ILK deletion probably reflects the combined effects of OPN upregulation along with defective survival signaling and altered cytoskeletal interactions, accounting for the increased severity compared to that seen with genetic manipulation of individual components of these pathways.

The potential clinical relevance of these observations is underscored by the association of human ILK mutations with cardiomyopathy[4]. Whether inflammation contributes to the clinical presentation in these patients or might be targeted for intervention has not been established and warrants additional investigation. Since OPN is secreted, measuring serum

levels in these patients would provide a practical next step in assessing OPN's potential contribution.

Supplementary Material

Refer to Web version on PubMed Central for supplementary material.

Acknowledgments

We thank Dr. Ling Li for technical support and Dr. Serafima Zaltsman for expertly managing the mouse colony. We thank Dr. Brian Hemmings for generously providing the Akt1 knockout mice[12].

Sources of Funding

This research was supported by a Leducq Foundation Network of Research Excellence (AR, JGS, CES) and grants from the NIH (JGS[NHLBI], AR[HL059521, HL094677], TM[HL098423], and JD[T32 HL073734]). AR also gratefully acknowledges support from Judith and David Ganz. SD was supported by grants from the Canadian Institutes for Health Research (CIHR), and the Canadian Cancer Society Research Institute (CCSRI)

References

1. Hannigan GE, Leung-Hagesteijn C, Fitz-Gibbon L, Coppolino MG, Radeva G, Filmus J, Bell JC, Dedhar S. Regulation of cell adhesion and anchorage-dependent growth by a new beta 1-integrin-linked protein kinase. Nature. 1996; 379:91–96. [PubMed: 8538749]
2. Legate KR, Montanez E, Kudlacek O, Fassler R. ILK, PINCH and parvin: the tIPP of integrin signalling. Nat Rev Mol Cell Biol. 2006; 7:20–31. [PubMed: 16493410]
3. Lu H, Fedak PW, Dai X, Du C, Zhou YQ, Henkelman M, Mongroo PS, Lau A, Yamabi H, Hinek A, Husain M, Hannigan G, Coles JG. Integrin-linked kinase expression is elevated in human cardiac hypertrophy and induces hypertrophy in transgenic mice. Circulation. 2006; 114:2271–2279. [PubMed: 17088456]
4. Knoll R, Postel R, Wang J, Kratzner R, Hennecke G, Vacaru AM, Vakeel P, Schubert C, Murthy K, Rana BK, Kube D, Knoll G, Schafer K, Hayashi T, Holm T, Kimura A, Schork N, Toliat MR, Nurnberg P, Schultheiss HP, Schaper W, Schaper J, Bos E, Den Hertog J, van Eeden FJ, Peters PJ, Hasenfuss G, Chien KR, Bakkers J. Laminin-alpha4 and integrin-linked kinase mutations cause human cardiomyopathy via simultaneous defects in cardiomyocytes and endothelial cells. Circulation. 2007; 116:515–525. [PubMed: 17646580]
5. Bendig G, Grimmler M, Huttner IG, Wessels G, Dahme T, Just S, Trano N, Katus HA, Fishman MC, Rottbauer W. Integrin-linked kinase, a novel component of the cardiac mechanical stretch sensor, controls contractility in the zebrafish heart. Genes Dev. 2006; 20:2361–2372. [PubMed: 16921028]
6. Wickstrom SA, Lange A, Montanez E, Fassler R. The ILK/PINCH/parvin complex: the kinase is dead, long live the pseudokinase! EMBO J. 2010; 29:281–291. [PubMed: 20033063]
7. White DE, Coutu P, Shi YF, Tardif JC, Nattel S, St Arnaud R, Dedhar S, Muller WJ. Targeted ablation of ILK from the murine heart results in dilated cardiomyopathy and spontaneous heart failure. Genes Dev. 2006; 20:2355–2360. [PubMed: 16951252]
8. Wang HV, Chang LW, Brixius K, Wickstrom SA, Montanez E, Thievessen I, Schwander M, Muller U, Bloch W, Mayer U, Fassler R. Integrin-linked kinase stabilizes myotendinous junctions and protects muscle from stress-induced damage. J Cell Biol. 2008; 180:1037–1049. [PubMed: 18332223]
9. Pereira JA, Benninger Y, Baumann R, Goncalves AF, Ozcelik M, Thurnherr T, Tricaud N, Meijer D, Fassler R, Suter U, Relvas JB. Integrin-linked kinase is required for radial sorting of axons and Schwann cell remyelination in the peripheral nervous system. J Cell Biol. 2009; 185:147–161. [PubMed: 19349584]
10. Lange A, Wickstrom SA, Jakobson M, Zent R, Sainio K, Fassler R. Integrin-linked kinase is an adaptor with essential functions during mouse development. Nature. 2009; 461:1002–1006. [PubMed: 19829382]

11. Peng X, Kraus MS, Wei H, Shen TL, Pariaut R, Alcaraz A, Ji G, Cheng L, Yang Q, Kotlikoff MI, Chen J, Chien K, Gu H, Guan JL. Inactivation of focal adhesion kinase in cardiomyocytes promotes eccentric cardiac hypertrophy and fibrosis in mice. J Clin Invest. 2006; 116:217–227. [PubMed: 16374517]
12. Yang ZZ, Tschopp O, Hemmings-Mieszczak M, Feng J, Brodbeck D, Perentes E, Hemmings BA. Protein kinase B alpha/Akt1 regulates placental development and fetal growth. J Biol Chem. 2003; 278:32124–32131. [PubMed: 12783884]
13. Chen WS, Xu PZ, Gottlob K, Chen ML, Sokol K, Shiyanova T, Roninson I, Weng W, Suzuki R, Tobe K, Kadowaki T, Hay N. Growth retardation and increased apoptosis in mice with homozygous disruption of the Akt1 gene. Genes Dev. 2001; 15:2203–2208. [PubMed: 11544177]
14. Liang X, Sun Y, Ye M, Scimia MC, Cheng H, Martin J, Wang G, Rearden A, Wu C, Peterson KL, Powell HC, Evans SM, Chen J. Targeted ablation of PINCH1 and PINCH2 from murine myocardium results in dilated cardiomyopathy and early postnatal lethality. Circulation. 2009; 120:568–576. [PubMed: 19652092]
15. Shai SY, Harpf AE, Babbitt CJ, Jordan MC, Fishbein MC, Chen J, Omura M, Leil TA, Becker KD, Jiang M, Smith DJ, Cherry SR, Loftus JC, Ross RS. Cardiac myocyte-specific excision of the beta1 integrin gene results in myocardial fibrosis and cardiac failure. Circ Res. 2002; 90:458–464. [PubMed: 11884376]
16. Kim JB, Porreca GJ, Song L, Greenway SC, Gorham JM, Church GM, Seidman CE, Seidman JG. Polony multiplex analysis of gene expression (PMAGE) in mouse hypertrophic cardiomyopathy. Science. 2007; 316:1481–1484. [PubMed: 17556586]
17. Satoh M, Nakamura M, Akatsu T, Shimoda Y, Segawa I, Hiramori K. Myocardial osteopontin expression is associated with collagen fibrillogenesis in human dilated cardiomyopathy. Eur J Heart Fail. 2005; 7:755–762. [PubMed: 16087132]
18. Rosenberg M, Zugck C, Nelles M, Juenger C, Frank D, Remppis A, Giannitsis E, Katus HA, Frey N. Osteopontin, a new prognostic biomarker in patients with chronic heart failure. Circ Heart Fail. 2008; 1:43–49. [PubMed: 19808269]
19. Renault MA, Robbesyn F, Reant P, Douin V, Daret D, Allieres C, Belloc I, Couffinhal T, Arnal JF, Klingel K, Desgranges C, Dos Santos P, Charpentier F, Gadeau AP. Osteopontin expression in cardiomyocytes induces dilated cardiomyopathy. Circ Heart Fail. 2010; 3:431–439. [PubMed: 20200330]
20. Abel ED, Kaulbach HC, Tian R, Hopkins JC, Duffy J, Doetschman T, Minnemann T, Boers ME, Hadro E, Oberste-Berghaus C, Quist W, Lowell BB, Ingwall JS, Kahn BB. Cardiac hypertrophy with preserved contractile function after selective deletion of GLUT4 from the heart. J Clin Invest. 1999; 104:1703–1714. [PubMed: 10606624]
21. Troussard AA, Mawji NM, Ong C, Mui A, St -Arnaud R, Dedhar S. Conditional knock-out of integrin-linked kinase demonstrates an essential role in protein kinase B/Akt activation. J Biol Chem. 2003; 278:22374–22378. [PubMed: 12686550]
22. Dai J, Li W, Chang L, Zhang Z, Tang C, Wang N, Zhu Y, Wang X. Role of redox factor-1 in hyperhomocysteinemia-accelerated atherosclerosis. Free Radic Biol Med. 2006; 41:1566–1577. [PubMed: 17045925]
23. Aoyama T, Matsui T, Novikov M, Park J, Hemmings B, Rosenzweig A. Serum and glucocorticoid-responsive kinase-1 regulates cardiomyocyte survival and hypertrophic response. Circulation. 2005; 111:1652–1659. [PubMed: 15795328]
24. Cook SA, Matsui T, Li L, Rosenzweig A. Transcriptional effects of chronic Akt activation in the heart. J Biol Chem. 2002; 277:22528–22533. [PubMed: 11956204]
25. Christodoulou DC, Gorham JM, Kawana M, DePalma SR, Herman DS, Wakimoto H. Quantification of gene transcripts with deep sequencing analysis of gene expression (DSAGE) using 1 to 2 microg total RNA. Curr Protoc Mol Biol. 2011; 25:25B.9.1–25B.9.16.
26. Audic S, Claverie JM. The Significance of Digital Gene Expression Profiles. Genome Res. 1997; 7:986–995. [PubMed: 9331369]
27. Whelan RS, Kaplinskiy V, Kitsis RN. Cell death in the pathogenesis of heart disease: mechanisms and significance. Annu Rev Physiol. 2010; 72:19–44. [PubMed: 20148665]

28. Ashkar S, Weber GF, Panoutsakopoulou V, Sanchirico ME, Jansson M, Zawaideh S, Rittling SR, Denhardt DT, Glimcher MJ, Cantor H. Eta-1 (osteopontin): an early component of type-1 (cell-mediated) immunity. Science. 2000; 287:860–864. [PubMed: 10657301]
29. Xie Z, Singh M, Singh K. Osteopontin modulates myocardial hypertrophy in response to chronic pressure overload in mice. Hypertension. 2004; 44:826–831. [PubMed: 15534078]
30. Graf K, Do YS, Ashizawa N, Meehan WP, Giachelli CM, Marboe CC, Fleck E, Hsueh WA. Myocardial osteopontin expression is associated with left ventricular hypertrophy. Circulation. 1997; 96:3063–3071. [PubMed: 9386176]
31. DeBosch B, Treskov I, Lupu TS, Weinheimer C, Kovacs A, Courtois M, Muslin AJ. Akt1 is required for physiological cardiac growth. Circulation. 2006; 113:2097–2104. [PubMed: 16636172]
32. Ashizawa N, Graf K, Do YS, Nunohiro T, Giachelli CM, Meehan WP, Tuan TL, Hsueh WA. Osteopontin is produced by rat cardiac fibroblasts and mediates A(II)-induced DNA synthesis and collagen gel contraction. J Clin Invest. 1996; 98:2218–2227. [PubMed: 8941637]
33. Singh K, Balligand JL, Fischer TA, Smith TW, Kelly RA. Glucocorticoids increase osteopontin expression in cardiac myocytes and microvascular endothelial cells. Role in regulation of inducible nitric oxide synthase. J Biol Chem. 1995; 270:28471–28478. [PubMed: 7499354]
34. Murry CE, Giachelli CM, Schwartz SM, Vracko R. Macrophages express osteopontin during repair of myocardial necrosis. Am J Pathol. 1994; 145:1450–1462. [PubMed: 7992848]
35. Caglayan E, Stauber B, Collins AR, Lyon CJ, Yin F, Liu J, Rosenkranz S, Erdmann E, Peterson LE, Ross RS, Tangirala RK, Hsueh WA. Differential roles of cardiomyocyte and macrophage peroxisome proliferator-activated receptor gamma in cardiac fibrosis. Diabetes. 2008; 57:2470–2479. [PubMed: 18511847]
36. Subramanian V, Krishnamurthy P, Singh K, Singh M. Lack of osteopontin improves cardiac function in streptozotocin-induced diabetic mice. Am J Physiol Heart Circ Physiol. 2007; 292:H673–H683. [PubMed: 16980342]
37. Deschamps AM, Spinale FG. Pathways of matrix metalloproteinase induction in heart failure: bioactive molecules and transcriptional regulation. Cardiovasc Res. 2006; 69:666–676. [PubMed: 16426590]
38. Philip S, Kundu GC. Osteopontin induces nuclear factor kappa B-mediated promatrix metalloproteinase-2 activation through I kappa B alpha /IKK signaling pathways, and curcumin (diferulolylmethane) down-regulates these pathways. J Biol Chem. 2003; 278:14487–14497. [PubMed: 12473670]
39. Rangaswami H, Bulbule A, Kundu GC. Nuclear factor-inducing kinase plays a crucial role in osteopontin-induced MAPK/IkappaBalpha kinase-dependent nuclear factor kappaB-mediated promatrix metalloproteinase-9 activation. J Biol Chem. 2004; 279:38921–38935. [PubMed: 15247285]
40. Gkretsi V, Mars WM, Bowen WC, Barua L, Yang Y, Guo L, St-Arnaud R, Dedhar S, Wu C, Michalopoulos GK. Loss of integrin linked kinase from mouse hepatocytes in vitro and in vivo results in apoptosis and hepatitis. Hepatology. 2007; 45:1025–1034. [PubMed: 17385211]
41. Hortelano S, Lopez-Fontal R, Traves PG, Villa N, Grashoff C, Bosca L, Luque A. ILK mediates LPS-induced vascular adhesion receptor expression and subsequent leucocyte trans-endothelial migration. Cardiovasc Res. 2010; 86:283–292. [PubMed: 20164118]
42. Assi K, Patterson S, Dedhar S, Owen D, Levings M, Salh B. Role of epithelial integrin-linked kinase in promoting intestinal inflammation: effects on CCL2, fibronectin and the T cell repertoire. BMC Immunol. 2011; 12:42. [PubMed: 21806815]

Cardiomyocyte-specific ILK deletion leads to a lethal cardiomyopathy characterized by cardiomyocyte death, fibrosis, and inflammation. Comprehensive profiling identifies ILK-dependent transcriptional effects and implicates osteopontin as a contributor to these phenotypes. The potential clinical relevance of these observations is underscored by the association of human ILK mutations with cardiomyopathy. Whether inflammation contributes to the clinical presentation in these patients or might be targeted for intervention has not been established and warrants additional investigation. Since OPN is secreted, measuring serum levels in these patients would provide a practical next step in assessing OPN's potential contribution.

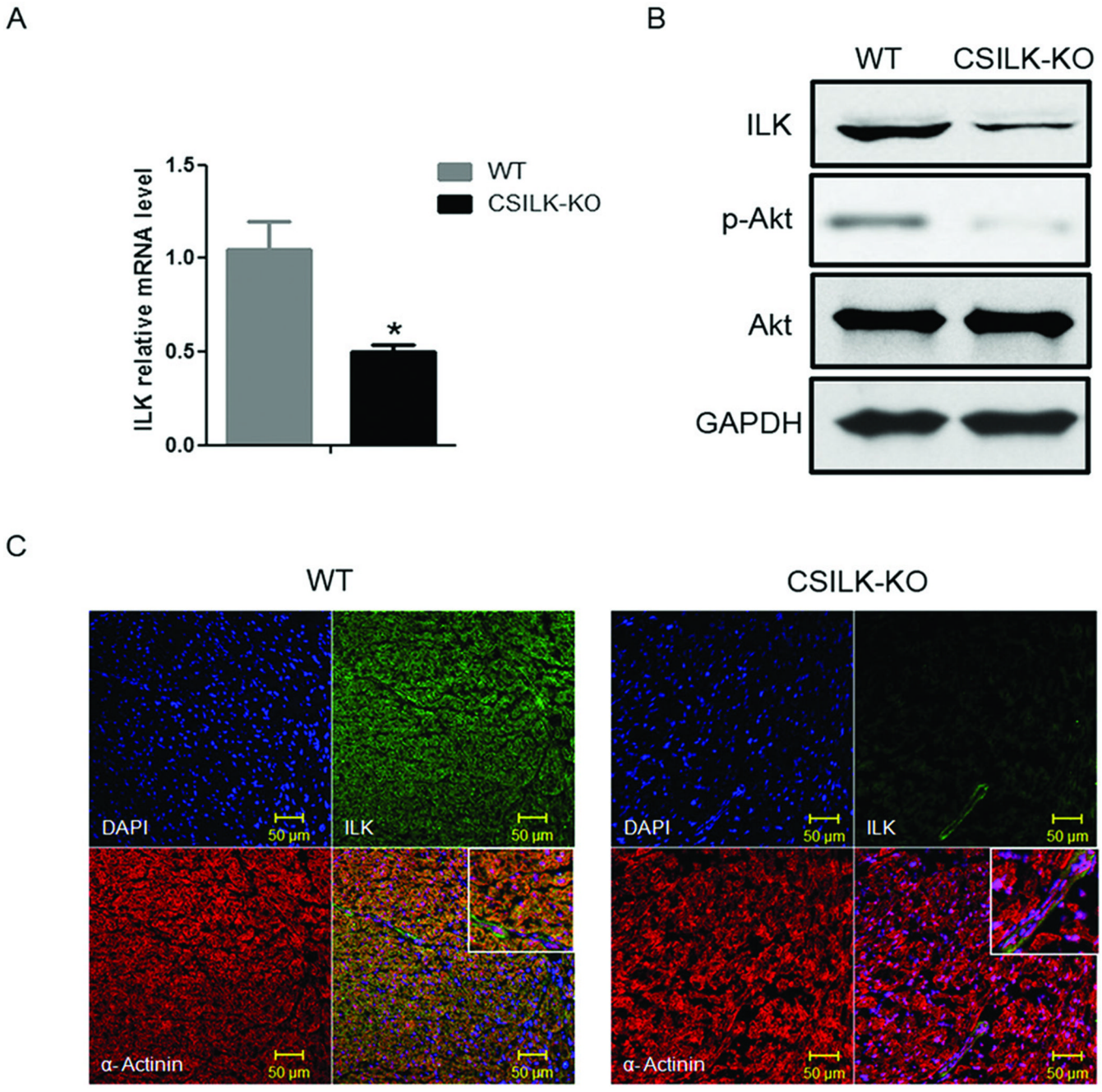

Figure 1. Cardiac Specific Deletion of ILK

Total RNA and protein were isolated from whole ventricles of 10 day old CSILK-KO and control littermates. (A) ILK mRNA expression was determined by QRT-PCR, $*p < 0.05$, n=5 in each genotype. (B) ILK protein expression was determined by immunoblotting. Results shown are representative of three independent experiments. (C) Immunofluorescence confocal microscopy shows virtually absent ILK staining in CSILK-KO cardiomyocytes identified by α-actinin staining but preserved vascular expression. Representative results from three independent experiments are shown.

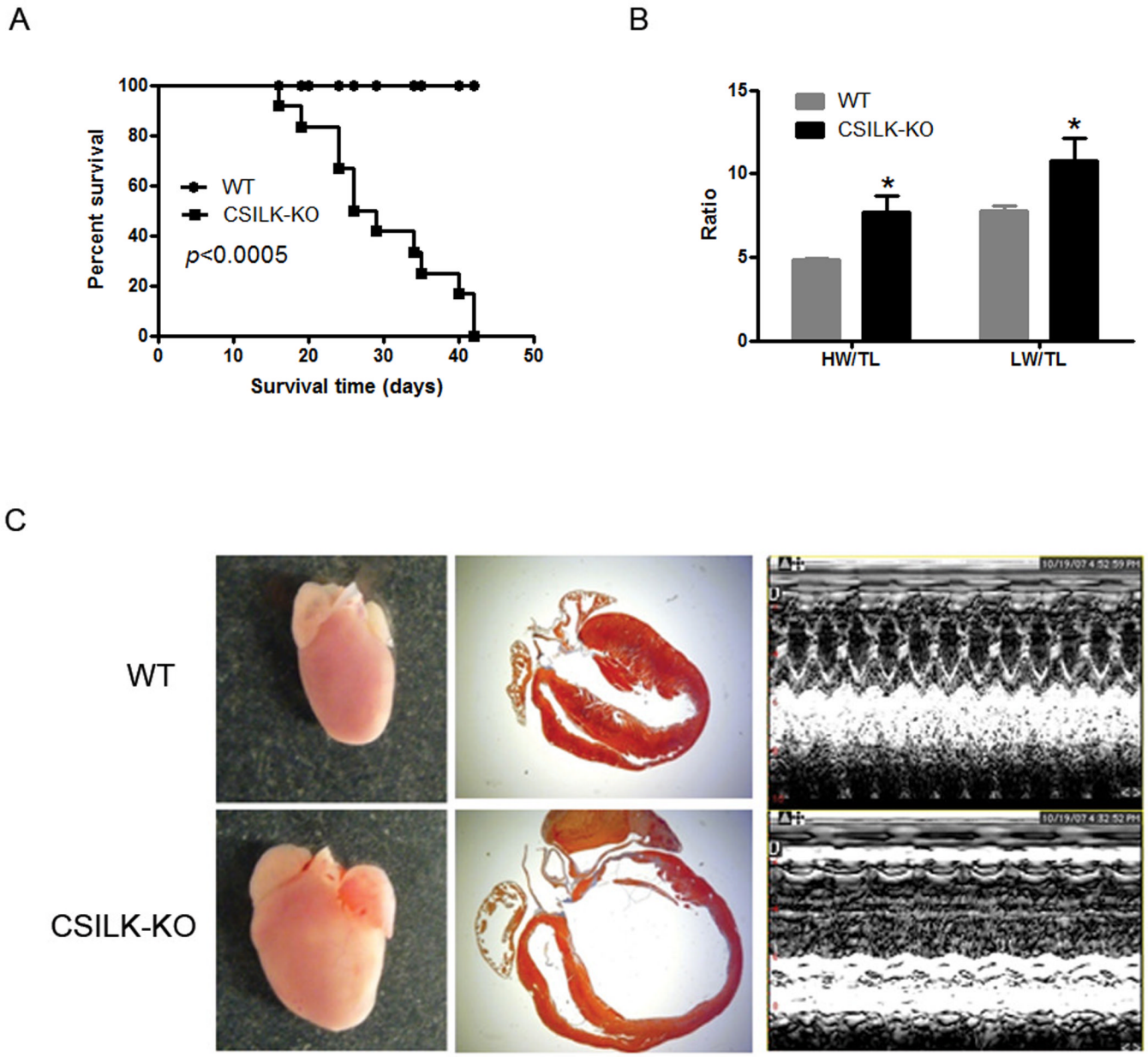

Figure 2. CSILK-KO cardiac phenotype

(A) Kaplan-Meier survival curves show early postnatal mortality among CSILK-KO which died by 3-6 weeks of age (n=12). (B) Both heart and lung weight normalized to tibial length were significantly increased compared with littermate controls, $*p < 0.05$, n=6. (C) Morphological and histological analyses of 21 day old CSILK-KO hearts show right and left ventricular chamber enlargement and wall thinning compared to control mice. Representative M-Mode echocardiograms are shown.

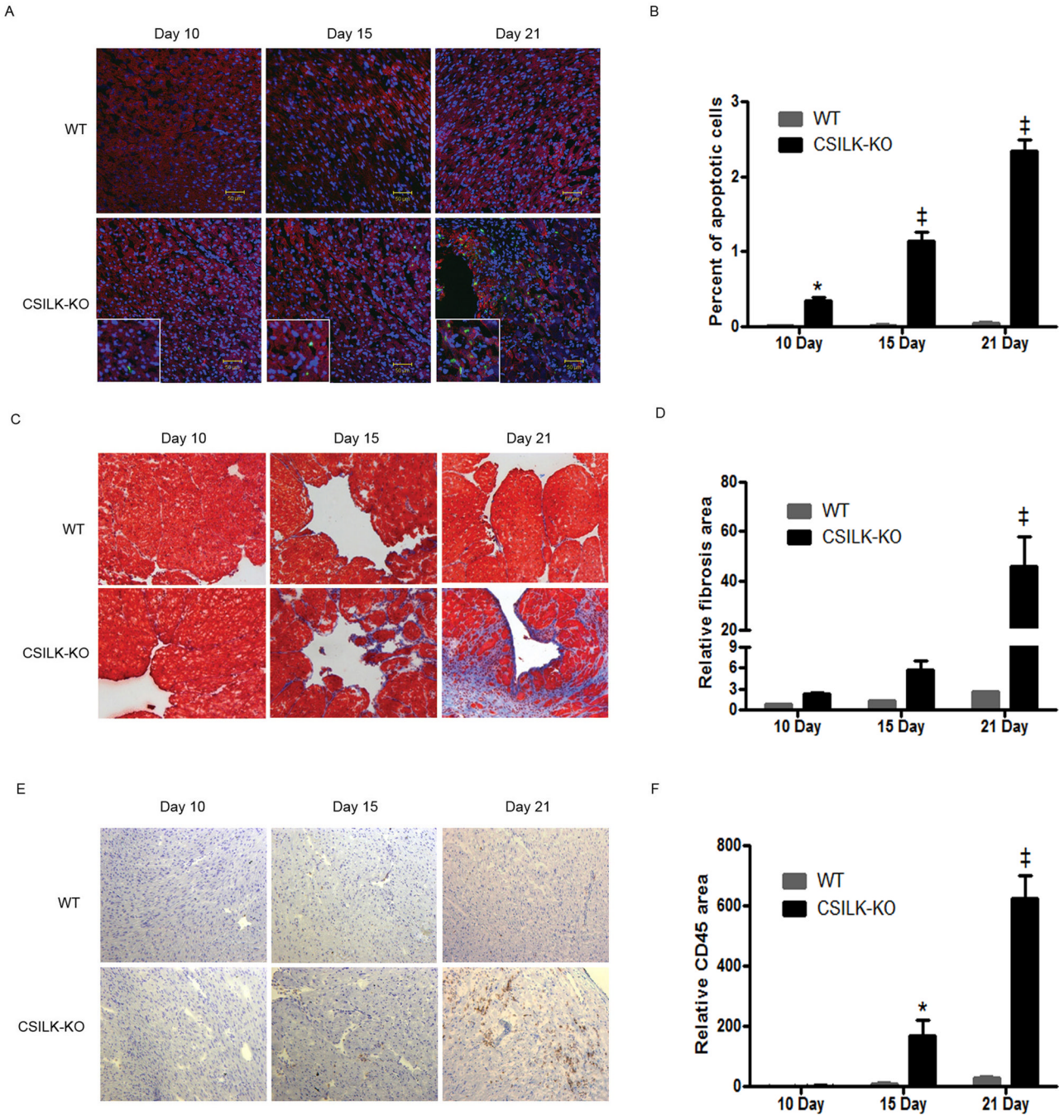

Figure 3. Increased apoptosis, fibrosis, and inflammation in CSILK-KO hearts

Representative TUNEL-stained (A), Masson's Trichrome-stained (C) or CD45-stained (E) cryosections of the heart from CSILK-KO mice and littermate controls at the indicated ages are shown, n=5 for each. Corresponding quantitative data are shown on the right panel, *$p <$ 0.05, ‡ $p < 0.001$ vs. WT at each time point, n=5 (B, D, F).

DSAGE

CSILK-KO	WT	KO/WT ratio	P value
63	29	2.17	2.71E-11
740	356	2.08	6.83E-106
138	64	2.16	1.92E-22
396	275	1.44	1.79E-18
132	63	2.10	8.12E-21
6	14	0.43	9.26E-04
39	24	1.63	2.69E-04
250	161	1.55	3.00E-16
172	28	6.14	3.37E-88
144	97	1.48	1.08E-08
10	21	0.48	1.09E-04
159	107	1.49	1.97E-09
1	5	0.20	4.87E-04
437	276	1.58	1.38E-29
19	34	0.56	2.27E-04
9	20	0.45	1.28E-04
81	38	2.13	1.39E-13
47	1	47.00	9.57E-45
93	61	1.52	1.80E-06
27	14	1.93	1.95E-04
25	9	2.78	1.25E-07
19	5	3.80	3.10E-08
19	4	4.75	9.97E-10
38	24	1.58	9.89E-04
20	10	2.00	5.28E-04

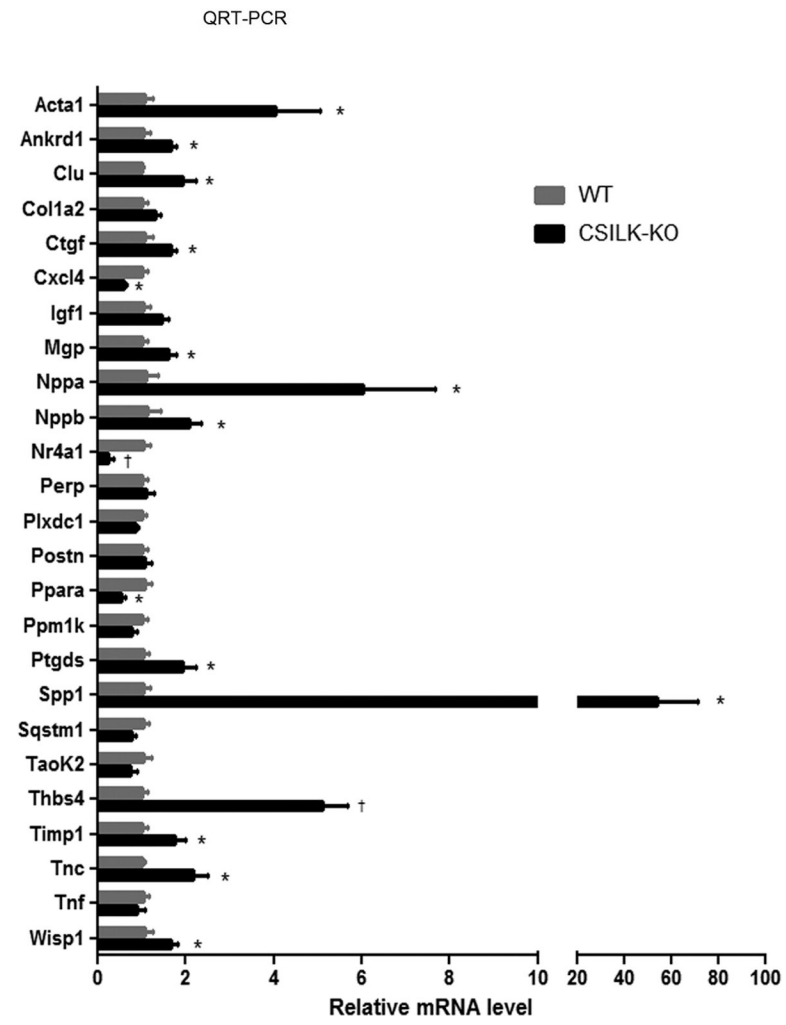

Figure 4. DSAGE analysis and validation

25 transcripts identified by DSAGE were independently assessed by QRT-PCR, and 16 of these DSAGE candidates have been confirmed at *p<0.05, †p<0.01, n=5.

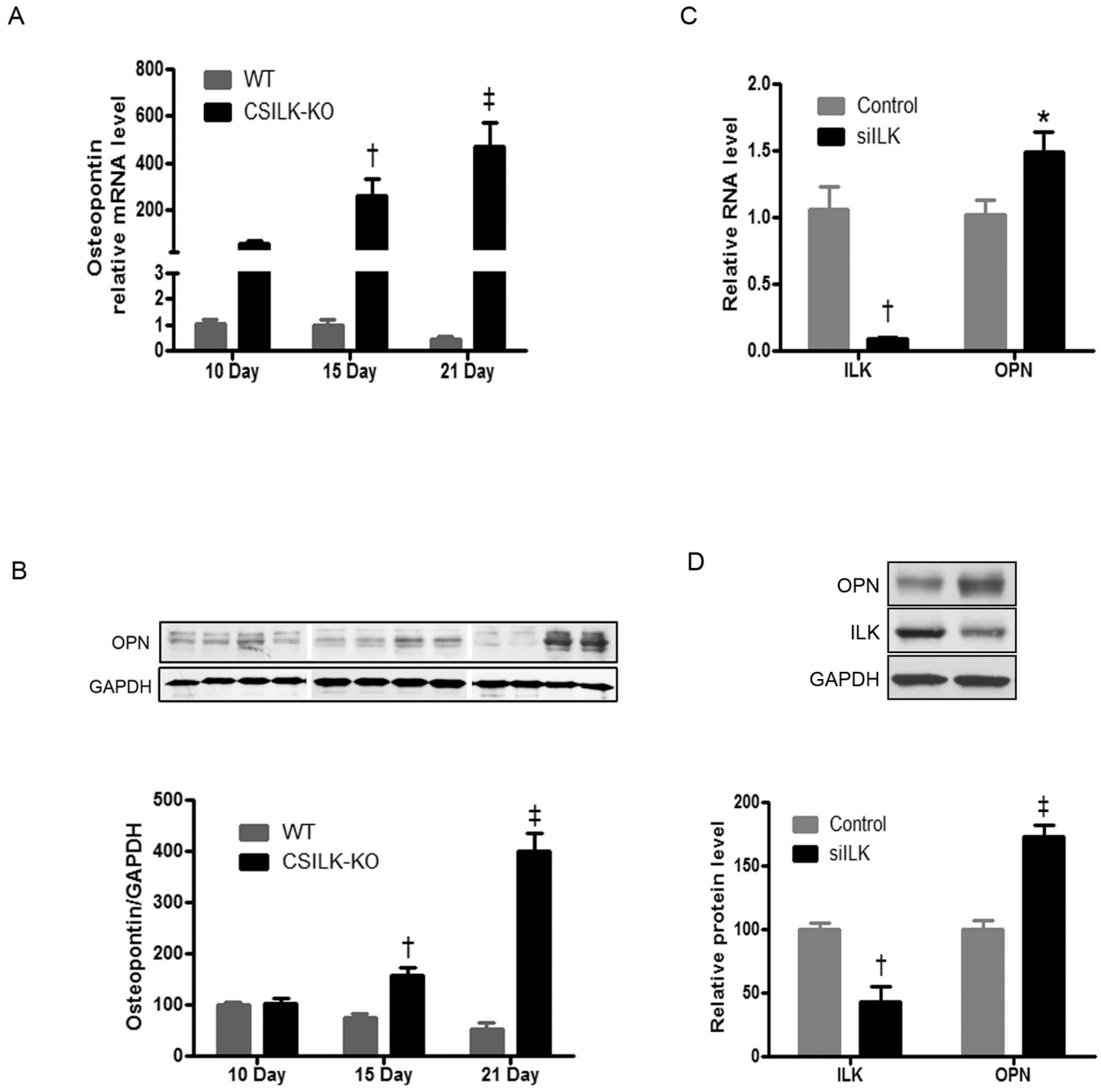

Figure 5. Cardiac OPN expression in CSILK-KO mice

OPN mRNA expression increased dramatically in CSILK-KO ventricles before the development of cardiac dysfunction, and continued to rise at post-natal days 15 and 21, †$p<0.01$, ‡ $p < 0.001$ vs. WT at each time point, n=5. (A). OPN protein level also increased early, significantly by 15 days and further at 21 days post-natal age in CSILK-KO hearts, †$p<0.01$, ‡ $p < 0.001$ vs. WT at each time point, n=5 in each group (B). siRNA-mediated depletion of ILK in rat neonatal cardiomyocytes leads to OPN mRNA (C) and protein, (D) expression increase, †$p<0.01$, ‡ $p < 0.001$ vs. control, n=5.

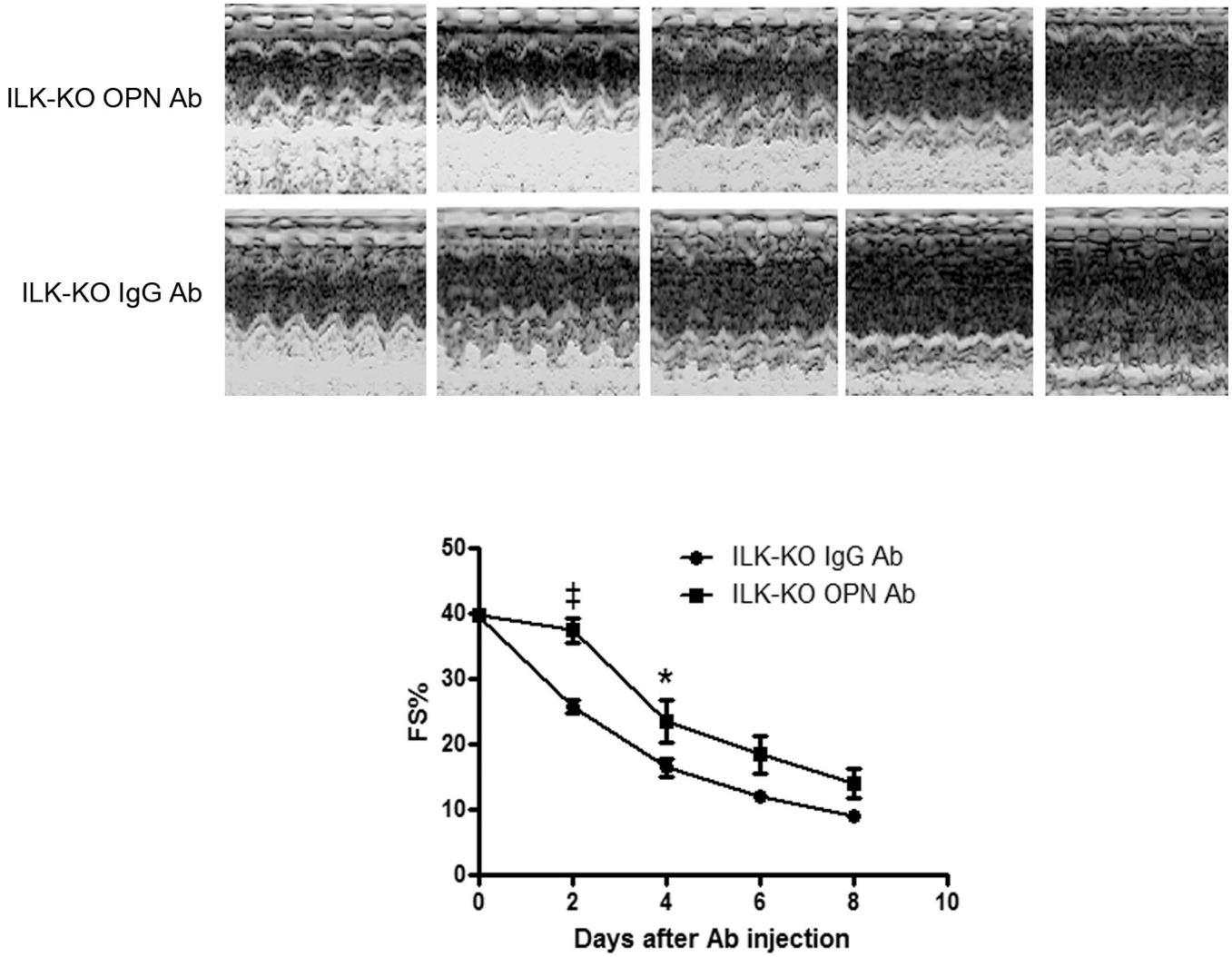

Figure 6. Anti-OPN antibody mitigates the functional decline in ILK-KO mice

Mice were treated with a neutralizing anti-mouse OPN IgG or control goat IgG every other day by intraperitoneal injection, starting from FS% is approximately 40%. All mice received echocardiographic assessment before each injection. M-mode echocardiographic analyses showed that inhibiting OPN mitigates the functional decline in ILK-KO mice. Representative M-mode echocardiograms from five independent experiments are shown. Corresponding quantitative data are shown on the lower panel, $*p < 0.05$, $‡p<0.001$ vs. control goat IgG injection at each time point, n=5.

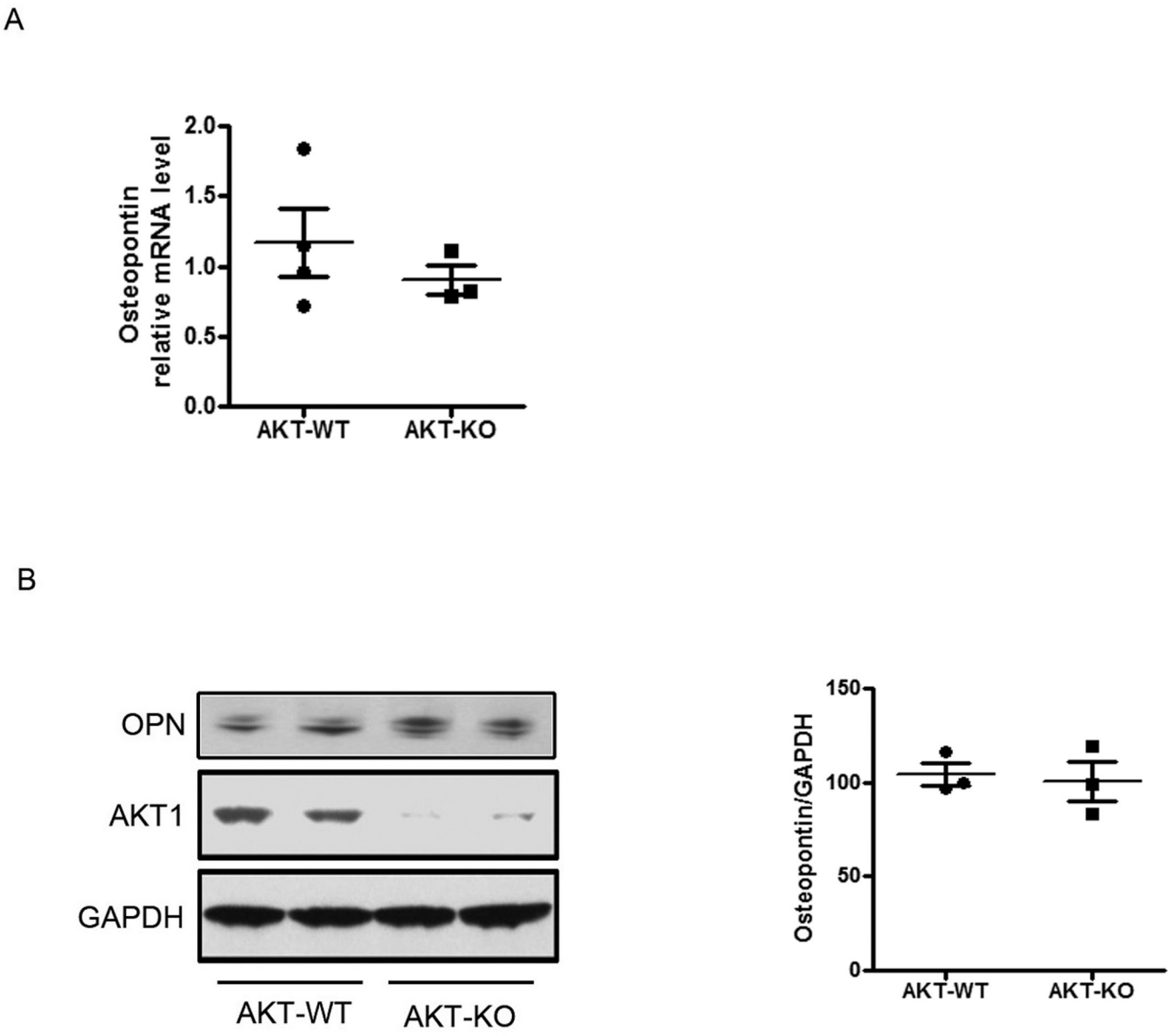

Figure 7. Akt1 does not regulate cardiac OPN expression

OPN mRNA (A) and protein expression (B) were not increased in Akt1 knockout hearts, n=3.

Table

Echocardiographic findings in CSILK-KO mice at different ages

	WT-Day10	CSILK-KO-Day10	WT-Day15	CSILK-KO-Day15	WT-Day21	CSILK-KO-Day21
IVSd	0.59±0.05	0.62±0.04	0.62±0.05	0.51±0.01	0.6±0.02	0.43±0.03*
LVDd	1.97±0.11	2.03±0.08	2.09±0.06	2.94±0.26†	2.16±0.1	4.11±0.22‡
LVPWd	0.66±0.06	0.68±0.03	0.74±0.03	0.71±0.08	0.69±0.04	0.55±0.02
IVSs	1.17±0.09	1.15±0.05	1.13±0.06	0.81±0.03†	1.16±0.05	0.58±0.06‡
LVDs	0.79±0.06	0.78±0.05	0.87±0.01	2.02±0.27‡	0.93±0.07	3.74±0.24‡
LVPWs	1.12±0.08	1.14±0.05	1.13±0.05	1.06±0.12	1.13±0.07	0.62±0.05‡
FS	60.07±1.52	61.28±1.38	58.4±0.92	31.78±4.09‡	57.08±1.43	8.91±2.12‡
HR	658.93±24.54	654.42±21.80	692.75±24.01	666.97±35.97	744.51±23.25	580.49±72.95*
Number	7	7	5	5	5	5

Comparisons between WT and CSILK-KO at each time point were performed using regular two-way ANOVA with Bonferroni post-tests.

*$p<0.05$,

†$p<0.01$,

‡$p<0.001$.

Abbreviations: IVSd, interventricular septum (end diastolic); LVDd, LV end-diastolic dimension; LVPWd, LV posterior wall (end diastolic); IVSs, interventricular septum (end systolic); LVDs, LV endsystolic dimension; LVPWs, LV posterior wall (end systolic); FS, fractional shortening. Number indicates number of mice.